

Microcompression study of Mg (0 0 0 1) single crystal

Erica Lilleodden

Institute of Materials Research, GKSS Research Center, Max-Planck-Strasse 1, 21502 Geesthacht, Germany

Received 1 August 2009; revised 29 December 2009; accepted 29 December 2009

Available online 4 January 2010

The stress–strain response, slip mechanisms and size effect in Mg (0 0 0 1) single crystal was investigated by microcompression testing. It is found that plasticity occurs relatively homogeneously up to a critical stress, at which point a massive deformation occurs. While the yield stress increases with decreasing diameter, the qualitative behavior is independent of column size. Cross-sectional electron back-scattered diffraction measurements show that twinning is not the predominant deformation mechanism. © 2009 Acta Materialia Inc. Published by Elsevier Ltd. All rights reserved.

Keywords: Magnesium; Compression test; Plastic deformation; Slip

The strong plastic anisotropy of Mg and its role as a structural material necessitate fundamental studies of its deformation mechanisms. Kelley and Hosford [1,2] provide possibly the best single crystal mechanical data for Mg single crystal, but even these experiments from 1968 were for the complicated stress state of channel die testing, where non-uniaxiality, friction and the potential for pre-existing internal twins or small-angle boundaries may obviate a reliable analysis of constitutive laws. Graff et al. [3] used Kelley and Hosford's data to identify crystal plasticity parameters for modeling polycrystalline deformation, but the validity and uniqueness of such constitutive laws is unproved. It is preferable to directly measure uniaxial stress–strain behavior, and identify the corresponding mechanisms of deformation.

One major challenge in this endeavor is the ability to obtain single-crystalline samples. This is especially true for Mg, where grown-in twins may control the mechanisms initiating plasticity. It is also important to fully characterize the deformation structure. To this end, microcompression testing [4,5] provides a great advantage over conventional testing approaches due to the small volume needed, which in turn allows more comprehensive characterization of the entire deformation volume through the use of various microscopic, diffraction or spectroscopic techniques.

A Mg single crystal of (0 0 0 1) orientation (purity 99.999%) was purchased from MaTecK GmbH. The crystal was mechanically polished, with a final mechan-

ical step of 50 nm SiO₂ slurry in a diluted solution of Pril® detergent and deionized water. A final etching step was used in order to remove some of the damage layer and to reveal the presence of any twins. Light microscopy revealed some patterning, which may be associated with twins or low-angle boundaries. Local regions of the crystals were then investigated with electron back-scattered diffraction to ensure that microcompression structures would be fabricated from single-crystalline volumes.

Microcompression columns were created from the bulk single crystal using focused ion beam (FIB) machining on an FEI Nanolab 200 DualBeam scanning electron FIB microscope. Annular cutting was employed with varying probe currents and cutting parameters that depend on the final desired geometry. Attempts were made to ensure a 3:1 aspect ratio of height to mid-plane diameter, and to minimize column taper. In any case where the ratio was greater than 4:1 or less than 2:1, the column was not used in the experiments. Due to the annular cutting method used, a slightly larger base diameter than top diameter will result, with a typical taper angle of 1.3° along the upper three-quarters of the column; an elliptical foot leads to a greater taper angle for the lower quarter of the column. Although this leads to some variation in axial stress along the column, the taper helps to stabilize the column if there is any misalignment between the microcolumn and the flat punch. A typical microcolumn of mid-plane diameter of 6.1 μm and its corresponding FIB machined cross-section is shown in Figure 1. Such a cross-sectional analysis of a sacrificial column is extremely helpful in assessing the true column geometry. If column taper is present or

E-mail: erica.lilleodden@gkss.de

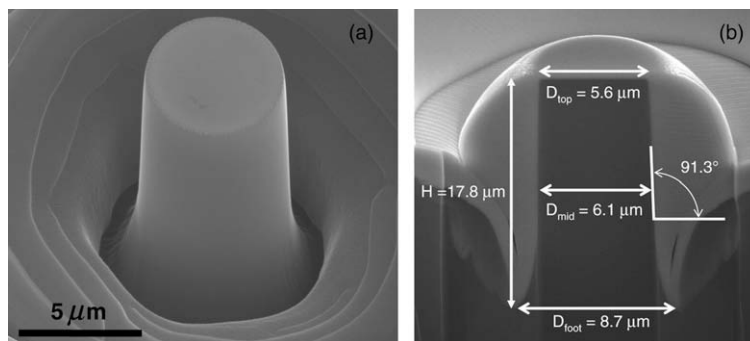


Figure 1. SEM micrographs showing (a) a 6.1 μm diameter column and (b) its corresponding FIB machined cross-section, showing the pre-deformation geometry of a typical column. The light gray corresponds to a protective Pt deposited prior to FIB cross-sectioning, the mid-gray corresponds to the redeposited Mg, and the dark gray corresponds to the Mg single crystal. Due to cutting through the Pt layer, the foot of the column appears slightly lighter than the single crystal; it is not redeposited material.

the base of the column is partially hidden due to surrounding material, a significant error in the height measurements can result. Such errors in geometry measurements can lead to significant inaccuracies in the analysis of stress and strain.

The compression experiments were conducted with a Nanoindenter XP (Agilent) equipped with a flat-ended conical indenter with a 15 μm diameter circular punch. Experiments were run to varying maximum strain using a nominally constant strain rate within the range of 0.0005 and 0.002 s^{-1} , with the majority of experiments run at 0.001 s^{-1} . The instrument is an inherently load-controlled instrument, and thus the displacement rate was controlled via feedback from the loading signal in order to achieve a specified strain rate.

An engineering stress–strain analysis of the load–displacement measurements is applied here, using the initial middle diameter and initial height of the column. Prior to using the usual equations to compute the stress and strain, the raw measurements of load and displacement are corrected for the Sneddon displacements due to elastic deformation in the material below the column, as well as the load–frame compliance due to machine and sample mount. A partial unloading segment was sometimes added to the loading profile so that an unloading stiffness could be directly measured at small strains in order to compute the elastic modulus. Initial seating between flat punch and column, along with incipient plasticity initiated prior to full yield, prevent an analysis of the elastic modulus from the initial loading response.

The engineering stress–strain curves associated with compression of two microcolumns of nominal diameter 6.1 μm are shown in Figure 2a. In both experiments, a partial unloading segment conducted at about 1% total strain shows an elastic modulus of 45 GPa, in good agreement with the expected value. It is clear that plasticity occurs prior to this unloading level, since unloading and loading curves are not superimposed. However, it is unclear whether such deformation can be considered full yield or whether small-scale localized plasticity during contact development accounts for the residual deformation. Nonetheless, a yield stress is defined in this study by a more significant slope change, which occurs during reloading at a stress level of about 170 MPa for both curves. We see that the two stress–strain curves

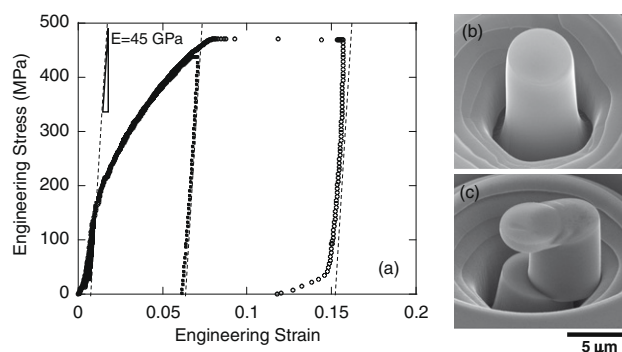


Figure 2. (a) Two engineering stress–strain curves for compression of two 6.1 μm columns. The dashed lines show a modulus of 45 GPa, as fitted to the partial unloading segments at around 1% strain, and drawn along the final unloading data for comparison. The post-compression structures associated with (b) compression of a column to 7% strain and (c) compression of a similar column to a critical stress of 485 MPa at which an inner section of the column sheared off.

track each other extremely well during continued loading, demonstrating the reproducibility of the 6.1 μm diameter columns.

One column was fully unloaded from a maximum stress of 445 MPa and strain of 7% and has an unloading slope of 45 GPa. The post-compression structure is shown in Figure 2b. The deformation is largely homogeneous along the column axis, with a slight asymmetric in-plane shearing. Figure 2c shows the post-compression structure of the second column, which was loaded to a maximum stress of 485 MPa. At this maximum stress, the column underwent a massive shear instability resulting in the outward displacement of a center section of the column; the top of the column and base section of the column remain nominally aligned with the original axis. This importantly reveals the critical, and largely underestimated, role that friction between the flat punch indenter and sample can play during microcompression testing. Obviously, the final unloading slope is not equivalent to the elastic modulus, since the extreme change in shape obviates such an analysis. The lower surface of the sheared-out volume is very planar and oriented with the basal plane, while the upper surface has undergone a tortuous shearing deformation, as indi-

cated by a thin, heavily deformed section of material connecting the top of the column to the mid-section.

All slip systems that include the basal plane or $\langle a \rangle$ Burgers vector have no resolved shear stress in the case of uniaxial compression along the (0001) direction. Only the pyramidal π_2 slip system with $\langle c+a \rangle$ Burgers vector has a non-zero Schmid factor. While Kelley and Hosford [1] state that even a slight misalignment of the c -axis can lead to sufficient resolved shear stress to initiate basal slip, the amount of in-plane shear displacement associated with the given axial compression would be significantly greater than what is observed should basal slip be a dominant mechanism. Therefore pyramidal π_2 slip and deformation twinning are the only possible mechanisms of deformation. In the case of π_2 slip, the symmetry of the (0001) loading axis leads to six equivalently stressed slip systems, which would easily account for the strong hardening observed.

In order to investigate the possibility of deformation twinning, electron back-scattered diffraction (EBSD) measurements were conducted on cross-sections of columns compressed to strains below the critical strain for massive shearing, such as the deformation associated with Figure 2(b). Figure 3 shows results from of a $10\ \mu\text{m}$ diameter column compressed to 5% axial plastic strain. It was found that no deformation twins are present. This is contrary to some claims that deformation twinning is the primary mechanism of deformation for c -axis compression in bulk single crystals [1,6–8]. There may be several reasons for the discrepancy. As previously discussed, it is difficult to obtain perfectly twin-free Mg on the bulk scale; the presence of small, pre-existing twins could provide potential sites for easier deformation twinning, circumventing costly nucleation. Differences in strain rate could also account for the differences between the studies, and is of interest for further research. Lastly, it is possible that a size effect in the twinning mechanism exists.

Multiple columns of varying diameter were investigated. Figure 4 shows the results from compression tests on columns of varying diameter from 2.1 to $10\ \mu\text{m}$. Three curves for each column diameter are presented. All show qualitatively the same deformation characteristics although a size effect in yield and flow stresses is observed. No twins were observed in any of the columns deformed to strains below the instability point. In the

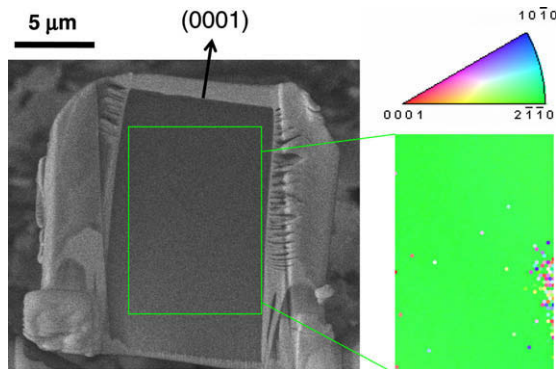


Figure 3. The cross-section of post-deformation column associated with pre-critical compression and its corresponding EBSD map showing no twin.

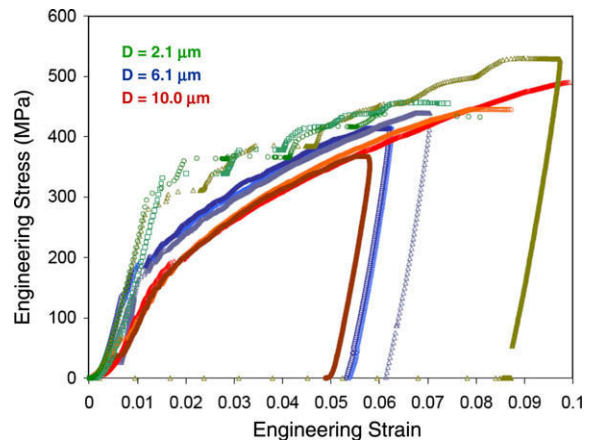


Figure 4. Multiple stress–strain curves for varying diameter columns (greens = $2.1\ \mu\text{m}$, blues = $6.1\ \mu\text{m}$, reds = $10\ \mu\text{m}$) showing a size effect in yield strength. Three experiments per size are shown. In some cases, a massive strain burst led to a final strain outside of the displayed limit.

case of columns deformed past the instability point where massive shearing occurred, some small twins were observed near the shearing surface. These are likely due to the complicated stress states resulting from the extreme change in geometry, and should not be considered as twinning under uniaxial compression. While the method for identifying the yield stress in these experiments can be debated, a clear size effect is observed through comparison of the 2.1 and $6\ \mu\text{m}$ diameter columns. We see that the yield stress of the $2.1\ \mu\text{m}$ diameter columns is about twice that of the $6.1\ \mu\text{m}$ diameter columns. Smaller is stronger. Such a size effect has been widely observed in microcompression studies of single crystals (e.g. [4,5,9–11]), though most studies have investigated face-centered cubic crystals. The yield point of the $10\ \mu\text{m}$ diameter columns is similar to that of the $6.1\ \mu\text{m}$ diameter columns although a greater initial loading compliance leads to an offset in strain. The source of this compliance could be greater seating between punch and sample, or more extensive microplasticity.

The stress–strain curves of the $2.1\ \mu\text{m}$ diameter columns show greater serrated-like flow, largely due to the smaller “ruler” associated with the computation of strain; any discrete bursts in displacement will appear as larger serrations in strain for columns of smaller height. Despite the serrated flow in the smallest columns, and an offset in stress due to the size-dependent flow stress, the hardening behavior appears nominally the same for all columns. This is not surprising since all columns undergo the same mechanism of deformation, namely slip on six equivalent pyramidal π_2 systems.

Independent of column size, massive shear instability, such as that shown in Figure 2c, occurs at stresses between 450 and 550 MPa. The value of critical stress or strain for this instability does not depend on column size. The position and thickness of the interior segment that shears out of the crystal appears to be stochastic. The direction in which it shears out of the column lines up crystallographically with the $[11\bar{2}0]$ directions, the so-called $\langle a \rangle$ slip directions, and is randomly distributed axially. That is to say that it is as likely that the shear occurs in the $\langle 11\bar{2}0 \rangle$ and $\langle \bar{1}\bar{1}20 \rangle$ directions. This

observation implies that the $\langle 0\ 0\ 0\ 1 \rangle$ compression axis is well aligned; otherwise the direction of massive shear would be identical for all columns.

Microcompression experiments on Mg $(0\ 0\ 0\ 1)$ single crystal revealed that:

1. twinning is not a relevant mechanism of deformation;
2. significant plasticity and hardening occurs, due to six active pyramidal π_2 slip systems;
3. a massive shear instability is reached, whereupon an interior segment of the column shears out of the column;
4. observations (1)–(3) are independent of column size;
5. a size effect is observed in the flow strength: flow strength increased with decreasing column diameter.

[1] E.W. Kelley, W.F. Hosford, *Trans. Metall. Soc.* 242 (1968) 5.

[2] E.W. Kelley, W.F. Hosford, *Trans. Metall. Soc.* 242 (1968) 654.

[3] S. Graff, D. Steglich, W. Brocks, *Intl. J. Plast.* 23 (2007) 1957.

[4] M.D. Uchic, D.M. Dimiduk, J.N. Florando, W.D. Nix, *Science* 305 (2004) 986.

[5] M.D. Uchic, D.M. Dimiduk, *Mat. Sci. Eng. A* 400–401 (2005) 268.

[6] E. Schmid, *Ztsch. Electrochem.* 37 (1931) 447.

[7] P.W. Bakarian, C.H. Mathewson, *Trans. AIME* 152 (1943) 226.

[8] R.E. Reed-Hill, W.D. Robertson, *Acta Metall.* 5 (1957) 717.

[9] D.M. Dimiduk, M.D. Uchic, T.A. Parthasarathy, *Acta Mater.* 53 (2005) 4065.

[10] J.R. Greer, W.D. Nix, *Phys. Rev. B* 73 (2006) 245410.

[11] C.V. Volkert, E.T. Lilleodden, *Philos. Mag.* 86 (2006) 5567.